ACS Sustainable Chemistry & Engineering

Research Article

pubs.acs.org/journal/ascecg

Graphene-Enhanced Oxygen Reduction by MN_4 Type Cobalt(III) Catalyst

Yashraj Gartia,[†,§] Charlette M. Parnell,[†,§] Fumiya Watanabe,[‡] Peter Szwedo,[†] Alexandru S. Biris,[‡] Nandan Peddi,[†] Zeid A. Nima,[‡] and Anindya Ghosh*[,†]

[†]Department of Chemistry, University of Arkansas at Little Rock, 2801 South University Avenue, Little Rock, Arkansas 72204, United States

[‡]Center for Integrative Nanotechnology Sciences, University of Arkansas at Little Rock, 2801 South University Avenue, Little Rock, Arkansas 72204, United States

Supporting Information

ABSTRACT: A nanocomposite of a dichloro-amido-macrocyclic cobalt(III) complex (**1**) and graphene was developed and characterized using various microscopic and spectroscopic techniques such as X-ray photoelectron spectroscopy, transmission electron microscopy, scanning electron microscopy and Raman spectroscopy. The nanocomposite was evaluated for electrocatalytic activity toward oxygen reduction reaction (ORR) in fuel cell applications. This complex (**1**) showed efficiency in a wide range of pH (acidic and basic) conditions for successful ORR. Apart from pH studies, the ratio of electrocatalyst **1** to graphene was varied for developing the optimal ORR catalyst. The use of graphene as a carbon support along with **1** in ORR studies not only resulted in increased current density but also a positive shift of the reduction potential by 140 mV (with respect to the Ag/AgCl reference electrode). Investigation of the catalytic mechanism using rotating disk electrode and rotating ring-disk electrode studies revealed its mechanism in acidic and basic conditions. The ORR was found to be a four-electron process in both pH conditions. The rate constant of ORR activity was found to be 3.85×10^5 $mol^{-1}s^{-1}$ at pH 2.0. The efficiency of the nanocomposite in ORR indicates the advantage of using both **1** and graphene for fuel cell applications.

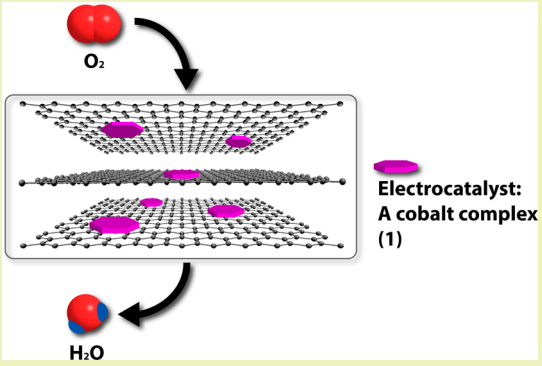

KEYWORDS: *Cobalt complex, electrocatalyst, graphene, oxygen reduction reaction, fuel cell*

INTRODUCTION

The electrochemical reduction of oxygen using hydrogen as a fuel is one of the most important electrochemical reactions today largely due to its encouraging potential as an energy solution.[1−6] Theoretically, these energy devices, also known as fuel cells, can serve as a more efficient way of producing energy as opposed to the present conventional energy-generating devices using fossil fuels.[7,8] This electrochemical reaction combines hydrogen with oxygen in a fuel cell to produce energy[9,10] with water being the reaction product. Hence, this is an environmentally clean, carbon-neutral process because it uses renewable resources to produce hydrogen.[11]

At the present, fuel cells depend on platinum (Pt), which is the most widely used metal as an electrochemical catalyst for oxygen reduction reaction (ORR) applications. However, the scarcity of Pt and its high cost have compelled scientists to either reduce the amount of Pt used or to look into the use of nonprecious metals as fuel cell catalysts. Cobalt and iron are two such non-noble metals that have been reported to be effective components in ORR catalysis. The use of these metals along with N_4-like sites has been proposed as an active catalyst for ORR. As a result, transition metal complexes, especially using macrocyclic rings with nitrogen pockets with either cobalt or iron, have attracted considerable interest as active catalysts for oxygen reduction. The macrocyclic ligand ring reported in this study has a similar framework attached to an aromatic ring. It is possible for us to change the pendent group present in the aromatic ring and, hence, affect the electronic structure and properties of the nitrogen pockets and the metal complex as a whole. Further alteration in the macrocyclic ring structure is also possible, which can contribute to further fine-tuning of the electronics of the active ORR catalyst. The complexation of these nitrogen-containing macrocyclic rings with nonprecious metals, such as iron, cobalt, etc., has provided us with a new class of catalysts with electrocatalytic activity. However, one parameter limiting the use of these complexes is their poor electroconductivity. Therefore, it would be ideal to include a conductive support to promote charge transfer, while at the same time increasing oxygen (O_2) diffusion and hydrogen (H_2) uptake[12] on the active site.

Received: September 11, 2014
Revised: November 23, 2014
Published: November 26, 2014

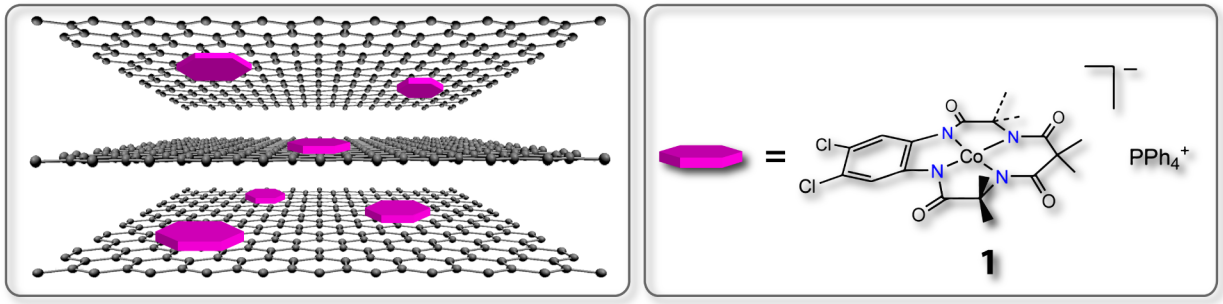

Figure 1. Cobalt(III)−amido-macrocyclic metal complex (**1**) (right) and the schematic representation of graphene composite of **1** used in this study for ORR.

Carbon nanotubes[13] and mesophorous carbon[14] have gained attention in ORR studies for their application as a carbon-based durable catalyst support. In addition to these carbon materials, several metal oxides, such as TiO_2,[15] SnO_2,[16] and NbO_x,[17] have also been used as catalyst supports. However, the cost of these carbon materials, along with the undesirable low conductivity and low surface area of the metal oxides, make these options less attractive.[18] Graphene nanomaterials, on the other hand, due to their low cost and their great mechanical strength, conductivity, and high surface area, have attracted both scientific and technological interest,[19] leading to their widespread application in various fields related to energy generation, conservation, and storage.

Graphene, as mentioned earlier, has excellent conductivity and high surface area, which makes it ideal for exploration as a support material to improve the electrolytic reduction of oxygen using new metal catalysts. In this research, we synthesized a new cobalt(III) amido-macrocyclic (MN_4) complex (**1**, Figure 1) with two electron withdrawing chlorine atoms as a pendent group on the aromatic ring attached to the two chelating N atom. This dichloro version of the macrocyclic cobalt(III) complex along with graphene showed a direct four-electron ORR process in a wide range of pH: 2.0 to 9.0 (Figure 1). We have reported the application of similar cobalt(III) complexes as fuel cell catalysts supported on multiwalled carbon nanotubes. However, this is the first report of the use of the dichloro version of these complexes particularly using highly efficient graphene as the support. The ORR activity of the new complex and the effect of graphene as support were studied based on our previous experience[20] and procedures described in the literature.[21−24] Interestingly, the use of graphene as carbon support increased the efficiency of the metal complex significantly. The peak potential at ORR occurred at a more positive potential when compared to previous nonprecious metal catalyst supported on graphene.[25,26]

EXPERIMENTAL SECTION

Reagents of analytical grade were bought from Aldrich Chemical Co., USA, or Fisher Scientific Company, USA and used without further modification unless otherwise noted. Graphene was purchased from Angstron Materials (N002-PDR Graphene Powder, 97% purity) and used as received. Transmission electron microscopy (TEM) and energy-dispersive X-ray spectroscopy (EDS) analysis were carried out using a JEOL TEM (JEM 2100F) instrument equipped with an EDAX Genesis EDS system. A Thermo Scientific Kα X-ray photoelectron spectroscopy (XPS) system was utilized to obtain the XPS spectra. Scanning electron microscopy (SEM) was carried out by using a JEOL SEM (JSM 7000F) instrument. Raman spectra were recorded using a Raman spectrometer (Horiba Jobin Yvon LabRam HR800, Edison, New Jersey) occupied by a He−Ne laser (17 mW) with wavelength of 784 nm and three Olympus BX-51 lenses with 100× micro-objectives magnitude connected to a Peltier-cooled CCD camera. The spectra were collected using 600 line/mm grating with the same acquisition time. In all measurements, the Raman spectrometer was calibrated using the Si−Si Raman signal, which is located at a 521 cm^{-1} Raman shift, and conducted at room temperature.

Ligand and Metal Complex Synthesis. The ligand was synthesized as previously described.[27] Synthesis of the cobalt(III) complex (**1**, Figure 1) was performed by reacting cobalt(II) chloride with the amido-macrocyclic ligand via deprotonation using *n*-butyllithium in THF (anhydrous). Overnight stirring produced an insoluble cobalt(II) complex, which was further exposed to the atmosphere to allowed oxidation to generate the purple cobalt(III) complex (**1**).

Electrochemical Studies. *General.* Cyclic voltammetry (CV) and rotating ring-disk voltammetry were conducted using a Pine Instruments (Raleigh, NC) bipotentiostat. A glassy carbon electrode was used as the working electrode during CV (Bioanalytical Systems, Lafayette, IN) and a graphite disk−platinum ring electrode and MSR speed control rotor were used during RRDE studies (Pine Instruments, Raleigh, NC). The reference electrode, Ag/AgCl, and counter electrode, platinum wire, were purchased from Pine Instruments and Bioanalytical Systems, respectively. A 100 mL glass vial equipped with a three-holed stopper was used as the electrochemical cell. Concentrated sulfuric acid was diluted to yield a 0.50 M H_2SO_4 solution with a calculated pH of 0.0. Buffer solutions of different pH (2.0, 4.0, 7.0, and 9.0) were prepared using a published procedure[28] and further diluted with deionized water. Unless otherwise noted, all buffer solutions used during the electrochemical ORR studies were saturated with oxygen. Furthermore, the buffer solutions were deoxygenated with high-purity nitrogen (Airgas) to check the electrochemical activity of complex **1**.[20] All experiments were conducted at room temperature (22 °C).

Preparation of Electrocatalyst. A homogeneous 1 mg/mL solution of Co composite was prepared by dissolving 5.0 mg of the catalyst in 5.0 mL of THF.[20] Various ratio mixtures (2:1, 1:1, 1:2) of catalyst to graphene were prepared and sonicated to yield a homogeneous suspension. This was followed by the addition of Nafion (5 wt %) and further sonication for 30 min. For CV and RRDE studies, a 10 μL aliquot of the mixture was drop casted on the glassy carbon electrode and dried under vacuum. When the composite was drop casted on the RRDE, care was taken to deposit the mixture on the disk portion (not the Pt ring) of the electrode. RDE polarization curves were recorded at various rotations (100, 400, 900, and 1600 rpm). The disk electrode recorded oxygen reduction while the ring electrode monitored any production of hydrogen peroxide (H_2O_2) by holding the potential at 1.0 V.

RESULTS AND DISCUSSION

XPS was performed to evaluate the binding energies of the atoms present in **1**. Several atoms are highlighted in Figure 2a.

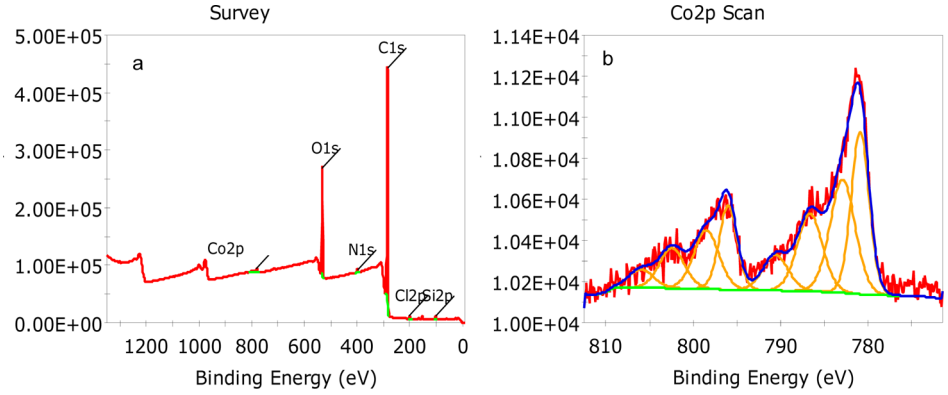

Figure 2. XPS spectra (a) survey scan of **1** supported on graphene and (b) Co 2p narrow scan peaks of **1**.

A narrow scan of the N atoms showed two peaks at 398.8 and 400.5 eV. The lower binding energy is due to the amide N,[29,30] while the higher binding energy is most likely from the interaction between the N atom and the carbons present in the graphene layers.[31] The oxygen atoms showed a peak at 532.7 eV, which can be attributed to the carbonyl oxygens within the complex.[32] A narrow scan of the carbon atoms showed three peaks between the range 284.8 and 289.1, which are attributed to the various carbon functional groups present within the complex and the graphene material.[33] A narrow scan of Co 2p (Figure 2b) showed four Co $2p_{3/2}$ peaks at 780.9, 783.3, 786.8, and 790.8 eV. There were four sets of satellite peaks observed, which could be accredited to possible photoreduction of **1** by X-rays to Co(II) during XPS analysis.[34] The peak separation between the two parental peaks at 780.9 and 796.1 eV matches well with a cobalt(III) complex.[34] The morphology of the composite was detected using TEM. From Figure 3, there

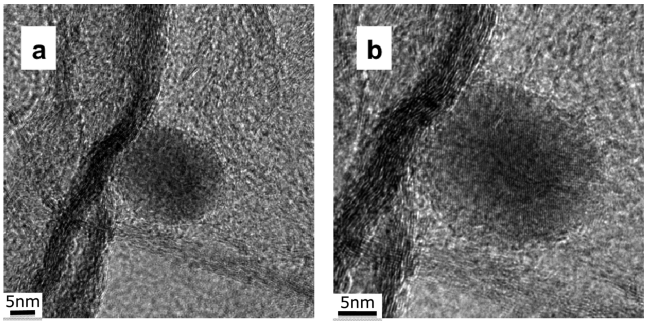

Figure 3. TEM images of **1** supported on graphene shown at (a) 300k× and (b) 500k× magnification.

appears to be leopard pattern-like decorations on the metallic nanoparticles attached to the graphene, which could be cobalt-complex/Nafion clusters (dark spots) with less than 2 nm diameter.

SEM images of the material (Supporting Information, Figure S1) are also presented and show the graphene nanomaterial throughout the composite. The graphene material shows crinkled pattern-like sheets and does not appear to restack on one another. Raman spectroscopy (Supporting Information, Figure S2) was further used to characterize electrocatalyst **1**–graphene nanocomposite (Supporting Information, Figure S2a) and compared with the pristine graphene material (Supporting Information, Figure S2b). The two bands at 1300 and 1600 cm^{-1} are characteristic of the D and G bands, respectively, present within graphene.[35] The D band is related to the breathing vibration modes of the defective six atom ring and the G band is related to Raman active modes (E_{2g}). In the presence of the electrocatalyst **1**, a new broad vibrational band at around 420 cm^{-1} was observed and it is indicative of the Co–N bonds that present in **1**.[36]

The ORR studies of the MN_4 type cobalt(III) complex (**1**) were performed to evaluate its ability to electrochemically reduce oxygen. The dichloro version of the macrocyclic complex was synthesized and used for the first time for its ORR activity (Figure 1). This complex was made water insoluble by exchanging the Li^+ counterion with PPh_4^+. The insoluble form along with Nafion was drop cast on the electrode for further ORR studies.

The complex **1** showed a small redox peak of the catalyst in nitrogen (N_2) saturated pH 2.0 buffer solution at 100 mV/s scan rate (Figure 4). Likewise, higher scan rates up to 1000

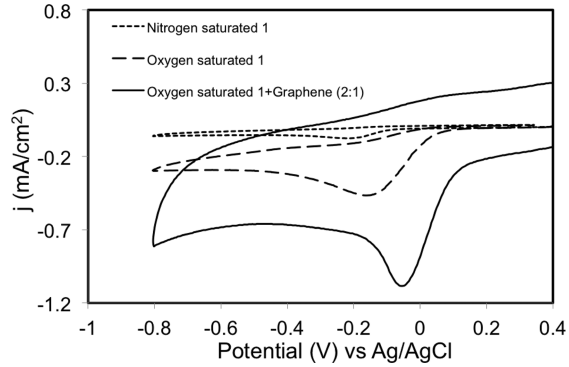

Figure 4. Cyclic voltammograms of the electrocatalyst **1** by itself in nitrogen and oxygen saturated pH 2.0 buffer, and the electrocatalyst **1** supported on graphene (2:1 ratio) in oxygen saturated pH 2.0 buffer.

mV/s showed low current density (Supporting Information, Figure S3). However, in O_2 saturated pH 2.0 buffer solution, complex **1** showed excellent reduction with a higher current and reduction peak at −0.15 V. On the other hand, graphene by itself showed no significant ORR activity (Supporting Information, Figure S4). Its response in saturated O_2 was only marginally increased, as compared to that in deaerated (N_2 saturated) solution. Interestingly, the use of electrocatalyst **1**, along with small amounts of graphene as conductive carbon support (2:1 ratio of **1**:graphene) (Figure 1b), not only more than doubled the current density but also showed an O_2 reduction peak at a more positive (less overvoltage) potential

dx.doi.org/10.1021/sc500589w | ACS Sustainable Chem. Eng. 2015, 3, 97–102

as compared to the electrocatalyst **1**, alone (Figure 4). The O_2 reduction was observed at −0.04 V at pH 2.0, which was a shift of +110 mV over **1** at the same buffer solution. A similar shift of +140 mV was also observed when the experiments were conducted at pH 4.0 (Supporting Information, Figure S5). Our earlier report[20] using multiwalled nanotubes with a similar MN_4 type Co complex revealed a much smaller shift of +40 mV. This higher efficiency could be attributed to the chemical nature of the electrocatalyst. Because the complex is planar and possesses a benzene ring, a source for π-electrons, and also contains four electron-rich nitrogen atoms, which have lone pair electrons, we speculate that the complex can easily attach to graphene surface via $\pi-\pi$ stacking interactions. These interactions scaffold the catalyst onto the graphene and give a more efficient material for ORR. The O_2 reduction of **1** supported on graphene occurred at a more positive potential than previously observed in a cobalt−porphyrin catalyst[25] (+26 mV shift) and an iron−polyphthalocyanine catalyst[26] (+40 mV shift), both supported on graphene (with respect to Ag/AgCl reference electrode). Interestingly, in both of these studies the use of graphene had also showed a positive shift in the ORR potential of about +136 and +106 mV, which demonstrates the enhancing property of graphene for ORR applications.

The effect of graphene as a conductive support for ORR was further evaluated by varying the ratio of **1** to graphene. Doubling the amount of graphene with respect to complex **1** (2:1 ratio of **1** to graphene) resulted in an increase in the ORR current density. Further increasing in the graphene concentration to 1:2 ratio of **1** to graphene led to an additional increase in current density (Figure 5). However, a small

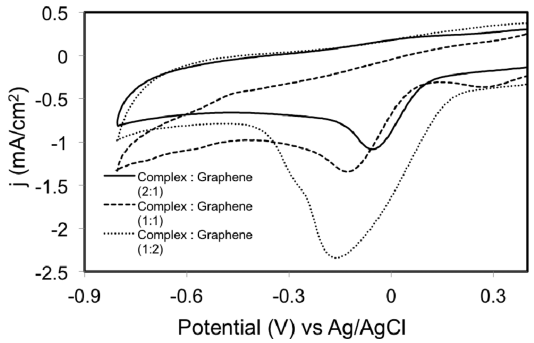

Figure 5. Cyclic voltammograms of complex **1** and graphene nanocomposite using different ratios of complex to graphene concentration in pH 2.0 buffer.

negative shift in the reduction potential was observed as the ratio of **1**:graphene was increased. Increasing the thickness of **1** + graphene/Nafion layer coatings using a sequential drop-casting technique showed a gradual increase in the current density (Supporting Information, Figure S6). However, no marked shift in the peak potential was observed as observed in our earlier work.[20]

The activity of **1** in different pH was also monitored for any changes in oxygen reduction potential. **1** showed activity in a wide range of pH: 2.0 to 9.0 (Figure 6). As the pH was decreased, a positive shift in the O_2 reduction peak was observed due to the increased availability of H^+. The current density nevertheless remained fairly constant.

For a better understanding of the mechanism of **1** in different pH as well as the **1** + graphene electrocatalyst system, the catalyst activity was studied using rotating disk electrode

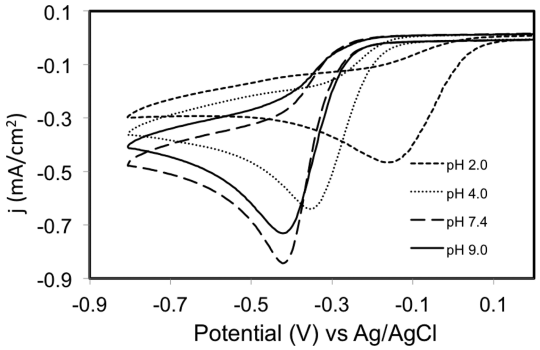

Figure 6. Cyclic voltammograms of complex **1** (mixed with Nafion) in oxygen saturated solutions of different pH at 25 °C.

(RDE), as well as the rotating ring disk electrode (RRDE) techniques. Figure 7a shows the rotating disk electrode reduction curves of 2:1 (**1**:graphene) at pH 2.0 at different rotation rates. No hydrogen peroxide (H_2O_2) was observed while studying the ring current and disk current at 100 rpm (Figure 7b), which was in accordance to our earlier work.[20]

From the RDE data, the observed limiting currents were used to construct the Koutecky−Levich equation in order to determine the number of electrons used in the ORR mechanism (Figure 8). This equation can be used to calculate the Levich (J_{lev}) and the kinetic currents (J_k):

$$1/J_{lim} = 1/J_{Lev} + 1/J_k$$

where $J_{Lev} = 0.620nFCD^{2/3}\omega^{1/2}\upsilon^{-1/6}$ (n = number of electrons transferred, F = Faraday constant, C = molar concentration of analyte, D = diffusion coefficient at 25 °C, ω = angular rotation rate of the electrode, and υ = kinematic viscosity of the solution at 25 °C); and J_k = rate of kinetically limited reaction.[20]

The slope of $1/0.620nFCD^{2/3}\upsilon^{-1/6}$ was obtained by plotting the graph between $1/J_{lim}$ and $\omega^{-1/2}$.[20] From the experimental, obtained from the Koutecky−Levich equation, and the theoretical plots (assuming n = 2 and n = 4), the number of electrons that were used in the experimental ORR process, was evaluated. This number was also calculated by RRDE data (Figure 7b) using the following equation:[20]

$$n = 4I_{disk}/(I_{disk} + I_{ring}/N)$$

Figure 8 shows the Koutecky−Levich plot of ORR at pH 2.0 using **1** + graphene (2:1), which gave an experimental value of 4.04 electrons. It was also noticed that the slopes from the experimental and theoretical value of n = 4 were closely matched. Additionally, RRDE showed no H_2O_2 evolution from the ring current, further coinciding with these results. Hence, oxygen reduction proves to be a four-electron process. Similarly, the Koutecky−Levich plot of ORR at higher pH of 9.0 (Supporting Information, Figure S7) was also found to show the ORR was also a four-electron process. The intercept of the experimental can be used to calculate the rate constant, k. The intercept represents the inverse of J_k, which equates to $10^3nFkC\Gamma$ where Γ is the molar concentration of the catalyst on the electrode (mol/cm^2). From the intercept, the calculated ORR rate constant was found to be 3.85×10^5 mol^{-1}s^{-1} at pH 2.0. This is a higher rate constant than that observed for carbon nanotubes, [20] which further indicates the utility of graphene in designing efficient ORR catalysts.

dx.doi.org/10.1021/sc500589w | ACS Sustainable Chem. Eng. 2015, 3, 97−102

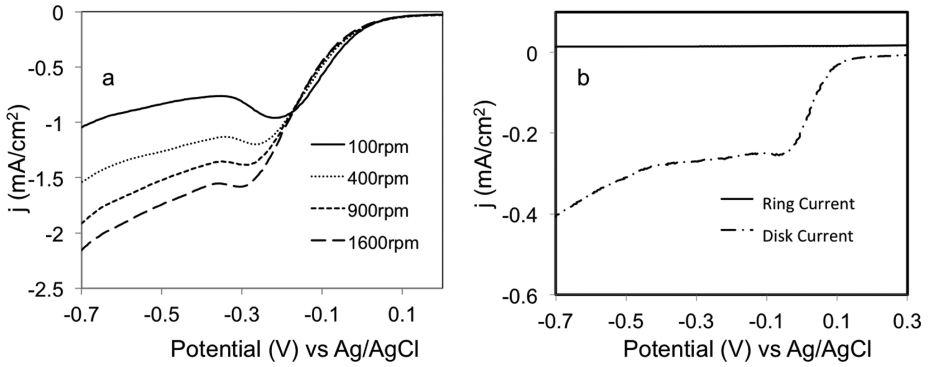

Figure 7. (a) RDE curves for the **1** + graphene (2:1) complex at pH 2.0 and 25 °C with increasing rpm speeds and (b) RRDE curves at 100 rpm holding ring potential at 1.0 V in oxygen saturated buffer solution (pH 2.0).

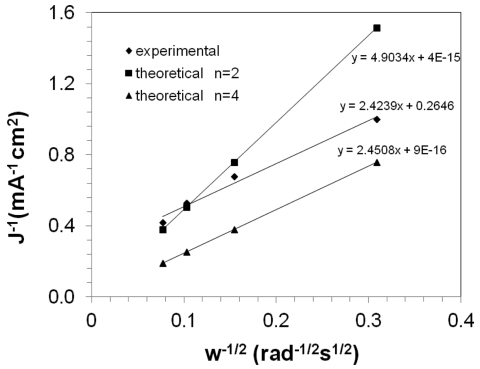

Figure 8. Koutecky–Levich plot of RDE of oxygen reduction using **1**+ graphene (2:1) at pH 2.0.

CONCLUSION

A dichloro version of an amido–cobalt(III) complex was synthesized and mixed with graphene at different ratios to develop a nanocomposite, which was used as a cathode catalyst for fuel cell applications. Various analytical techniques, such as XPS, were performed to characterize the nanocomposite. TEM and SEM analyses revealed the morphology of the nanocomposite material and showed a leopard-like pattern of **1** on the surface of graphene. Raman spectroscopy showed the presence of a new vibrational band, when compared to the graphene material, which was identified as the cobalt–nitrogen bond found within **1**. The catalytic activity of the nanocomposite of **1** and graphene was studied electrochemically for oxygen reduction. It was observed that increasing ratio of catalyst to graphene from 1:1 to 1:2 gave higher overall current density. Additionally, increased current density was observed as the layers of the nanocomposite of **1** and graphene increased on the electrode surface. The nanocomposite of **1** and graphene not only increased the current density but also shifted the ORR peak potential by +140 mV when compared to **1** in the absence of graphene. Alone, graphene showed almost no activity toward ORR. However, when mixed with **1**, the nanocomposite of **1** and graphene becomes a more effective material for ORR. The electrocatalytic activity and mechanism for ORR were also studied in several pH conditions and found to be a four-electron reduction process. The rate constant for oxygen reduction was determined to be 3.85×10^5 $mol^{-1}s^{-1}$ at pH 2.0. The catalyst system also showed higher ORR catalytic activity and current density compared to our previous reports with multiwalled carbon nanotubes. Graphene increased the efficiency of the metal complex significantly, proving it to be superior to other carbonaceous nanomaterials such as carbon nanotubes, while the metal complex proved superior in ORR activity in comparison other similar nonprecious MN_4 metal catalysts.

ASSOCIATED CONTENT

Supporting Information

SEM images, Raman spectra, additional cyclic voltammetry, RDE, and RRDE for the electrocatalyst. This material is available free of charge via the Internet at http://pubs.acs.org.

AUTHOR INFORMATION

Corresponding Author

*A. Ghosh. E-mail: axghosh@ualr.edu. Phone: 501 569 8827. Fax: 501 569 8838.

Author Contributions

§These authors contributed equally in the preparation of this paper.

Notes

The authors declare no competing financial interest.

ACKNOWLEDGMENTS

A.G. and A.S.B thank the National Science Foundation (Grant CHE-1229149) major research instrument grant to complete this work. The editorial assistance of Dr. Marinelle Ringer is also acknowledged.

REFERENCES

(1) Jacobson, M.; Colella, W.; Golden, D. Cleaning the air and improving health with hydrogen fuel-cell vehicles. *Science* **2005**, *308* (5730), 1901–1905.

(2) Schultz, M. G.; Diehl, T.; Brasseur, G. P.; Zittel, W. Air pollution and climate-forcing impacts of a global hydrogen economy. *Science* **2003**, *302* (5645), 624–627.

(3) Dusatre, V. Materials for clean energy. *Nature* **2001**, *414*, 345–352.

(4) Martin, R.; Buchwald, S. L. Pd-catalyzed Kumada-Corriu cross-coupling reactions allowed the use of Knochel-type Grignard reagents. *J. Am. Chem. Soc.* **2007**, *129* (13), 3844–3845.

(5) Dias, H. V. R.; Browning, R. G.; Polach, S. A.; Diyabalanage, H. V. K.; Lovely, C. J. Activation of alkyl halides via a silver-catalyzed carbene insertion process. *J. Am. Chem. Soc.* **2003**, *125* (31), 9270–9271.

(6) Brumfiel, G. Hydrogen cars fuel debate on basic research. *Nature* **2003**, *422*, 104.

(7) Bashyam, R.; Zelenay, P. A class of non-precious metal composite catalysts for fuel cells. *Nature* **2006**, *443* (7107), 63–66.

(8) Berger, D. J. Fuel cells and precious-metal catalysts. *Science (Washington, DC, U. S.)* **1999**, *286*, 49.
(9) Carrette, L.; Friedrich, K. A.; Stimming, U. Fuel cells - Fundamentals and applications. *Fuel Cells* **2001**, *1* (1), 5−39.
(10) Costamagna, P.; Srinivasan, S. Quantum jumps in the PEMFC science and technology from the 1960s to the year 2000 Part II. Engineering, technology development and application aspects. *J. Power Sources* **2001**, *102* (1−2), 253−269.
(11) Dani, P.; Karlen, T.; Gossage, R. A.; Gladiali, S.; Van Koten, G. Hydrogen-transfer catalysis with pincer-aryl ruthenium(II) complexes. *Angew. Chem., Int. Ed.* **2000**, *39* (4), 743−745.
(12) Ghosh, A.; Subrahmanyam, K. S.; Krishna, K. S.; Datta, S.; Govindaraj, A.; Pati, S. K.; Rao, C. N. R. Uptake of H_2 and CO_2 by graphene. *J. Phys. Chem. C* **2008**, *112* (40), 15704−15707.
(13) Wu, G.; Xu, B. Carbon nanotube supported Pt electrodes for methanol oxidation: A comparison between multi- and single-walled carbon nanotubes. *J. Power Sources* **2007**, *174* (1), 148−158.
(14) Shao, Y.; Zhang, S.; Kou, R.; Wang, X.; Wang, C.; Dai, S.; Viswanathan, V.; Liu, J.; Wang, Y.; Lin, Y. Noncovalently functionalized graphitic mesoporous carbon as a stable support of Pt nanoparticles for oxygen reduction. *J. Power Sources* **2010**, *195* (7), 1805−1811.
(15) Huang, S.; Ganesan, P.; Park, S.; Popov, B. N. Development of a Titanium Dioxide-Supported Platinum Catalyst with Ultrahigh Stability for Polymer Electrolyte Membrane Fuel Cell Applications. *J. Am. Chem. Soc.* **2009**, *131* (39), 13898−13899.
(16) Saha, M. S.; Li, R.; Cai, M.; Sun, X. High electrocatalytic activity of platinum nanoparticles on SnO2 nanowire-based electrodes. *Electrochem. Solid-State Lett.* **2007**, *10* (8), B130−B133.
(17) Sasaki, K.; Zhang, L.; Adzic, R. R. Niobium oxide-supported platinum ultra-low amount electrocatalysts for oxygen reduction. *Phys. Chem. Chem. Phys.* **2008**, *10* (1), 159−167.
(18) Shao, Y.; Liu, J.; Wang, Y.; Lin, Y. Novel catalyst support materials for PEM fuel cells: current status and future prospects. *J. Mater. Chem.* **2009**, *19* (1), 46−59.
(19) Geim, A. K.; Novoselov, K. S. The rise of graphene. *Nat. Mater.* **2007**, *6* (3), 183−191.
(20) Nasini, U. B.; Gartia, Y.; Ramidi, P.; Kazi, A.; Shaikh, A. U.; Ghosh, A. Oxygen reduction reaction catalyzed by cobalt(III) complexes of macrocyclic ligands supported on multiwalled carbon nanotubes. *Chem. Phys. Lett.* **2013**, *566*, 38−43.
(21) Orellana, W. Catalytic activity toward oxygen reduction of transition metal porphyrins covalently linked to single-walled carbon nanotubes: A density functional study. *Phys. Rev. B* **2011**, *84* (15), 155405.
(22) Qu, J.; Shen, Y.; Qu, X.; Dong, S. Electrocatalytic reduction of oxygen at multi-walled carbon nanotubes and cobalt porphyrin modified glassy carbon electrode. *Electroanalysis* **2004**, *16* (17), 1444−1450.
(23) Baskaran, D.; Mays, J. W.; Zhang, X. P.; Bratcher, M. S. Carbon nanotubes with covalently linked porphyrin antennae: Photoinduced electron transfer. *J. Am. Chem. Soc.* **2005**, *127* (19), 6916−6917.
(24) Murakami, H.; Nomura, T.; Nakashima, N. Noncovalent porphyrin-functionalized single-walled carbon nanotubes in solution and the formation of porphyrin−nanotube nanocomposites. *Chem. Phys. Lett.* **2003**, *378* (5−6), 481−485.
(25) Jiang, L.; Cui, L.; He, X. Cobalt-porphyrin noncovalently functionalized graphene as nonprecious-metal electrocatalyst for oxygen reduction reaction in an alkaline medium *J. Solid State Electrochem.* **2014**, DOI: 10.1007/s10008-014-2628-3.
(26) Lin, L.; Li, M.; Jiang, L.; Li, Y.; Liu, D.; Cui, L.; Cui, L. A novel iron(II) polyphthalocyanine catalyst assembled on graphene with significantly enhanced performance for oxygen reduction reaction in alkaline medium. *J. Power Sources* **2014**, *268*, 269−278.
(27) Ghosh, A.; Ramidi, P.; Pulla, S.; Sullivan, S.; Collom, S.; Gartia, Y.; Munshi, P.; Biris, A. S.; Noll, B. C.; Berry, B. C. Cycloaddition of CO_2 to epoxides using a highly active Co(III) complex of tetraamidomacrocyclic ligand. *Catal. Lett.* **2010**, *137* (1), 1−7.
(28) Carmody, W. R. Easily prepared wide range buffer series. *J. Chem. Educ.* **1961**, *38* (11), 559.
(29) Truica-Marasescu, F.; Wertheimer, M. R. Nitrogen-rich plasma-polymer films for biomedical applications. *Plasma Process. Polym.* **2008**, *5* (1), 44−57.
(30) Beamson, G.; Briggs, H. *High resolution XPS of organic polymers: The Scienta ESCA 300 database*; Wiley: Chichester, U. K., 1992.
(31) Kruusenberg, I.; Matisen, L.; Tammeveski, K. Oxygen Electroreduction on multi-walled carbon nanotube supported metal phthalocyanines and porphyrins in acid media. *Int. J. Electrochem. Sci.* **2013**, *8*, 1057−1066.
(32) Lopez, G. P.; Castner, D. G.; Ratner, B. D. XPS O 1s binding energies for polymers containing hydroxyl, ether, ketone and ester groups. *Surf. Interface Anal.* **1991**, *17* (5), 267−272.
(33) Miller, D. J.; Biesinger, M. C.; McIntyre, N. S. Interaction of CO_2 and CO at fractional atmosphere pressures with iron and iron oxide surfaces: One possible mechanism for surface contamination? *Surf. Interface Anal.* **2002**, *33* (4), 299−305.
(34) Tufts, B. J.; Abrahams, I. L.; Caley, C. E.; Lunt, S. R.; Miskelly, G. M.; Sailor, M. J.; Santangelo, P. G.; Lewis, N. S.; Lawrence Roe, A.; Hodgson, K. O. XPS and EXAFS studies of the reactions of cobalt(III) ammine complexes with gallium arsenide surfaces. *J. Am. Chem. Soc.* **1990**, *112* (13), 5123−5136.
(35) Hodkiewicz, J. *Characterizing graphene with raman spectroscopy*; Application Note No. 51946; Thermo Fisher Scientific: Madison, WI, 2010.
(36) Nayak, S. C.; Das, P. K.; Sahoo, K. K. Synthesis and characterization of some cobalt(III) complexes containing heterocyclic nitrogen donor ligands. *Chem. Pap.* **2003**, *57* (2), 91−96.